RSC Advances

PAPER

View Article Online
View Journal | View Issue

Cite this: *RSC Adv.*, 2020, **10**, 18384

Phomretones A–F, C_{12} polyketides from the co-cultivation of *Phoma* sp. YUD17001 and *Armillaria* sp.†

Hong-Tao Li, Tao Liu, Ruining Yang, Fei Xie, Zhi Yang, Yabin Yang, Hao Zhou* and Zhong-Tao Ding*

Received 18th March 2020
Accepted 4th May 2020

DOI: 10.1039/d0ra02524k

rsc.li/rsc-advances

Six new C_{12} polyketides, phomretones A–F (**1–6**), were isolated from the co-culture of *Armillaria* sp. and the endophytic fungus *Phoma* sp. YUD17001 associated with *Gastrodia elata*. Neither fungus produced these compounds when cultured alone. The structures of **1–6** were established on the basis of comprehensive spectroscopic analyses, while their absolute configurations were determined by the comparsion of experimental and calculated ECD spectra. Compounds **2–4** are diastereoisomers of each other and featured high levels of stereoisomerization and oxidation.

Introduction

Co-cultivation of microorganisms attracts substantial attention from both chemists and biologists as the activation of silent biosynthetic pathways can be utilized for the isolation and characterization of structurally novel and biologically meaningful molecules.[1–4] Hitherto, co-culture systems have been developed with various microorganisms, including bacterium–fungus, bacterium–bacterium, bacterium–protist, archaea–fungus and fungus–fungus co-cultures, involving both budding and filamentous forms.[2] Examples of the production of previously unknown secondary metabolites by co-culture include the penixylarins A–B,[4] fusatricinones A–D,[5] cytochathiazines,[6] berkeleylactones,[7] libertellenones,[8] tetrapeptides,[9] and the citrifelins.[10]

As part of our ongoing study of metabolites produced by fungal co-cultures,[11–13] we analyzed the co-culture of the endophytic fungus *Phoma* sp. YUD17001 and the symbiotic fungus *Armillaria* sp. associated with *Gastrodia elata*. This led to the isolation of two phenolic, phexandiols A and B, and three aliphatic ester derivatives, phomesters A–C.[11] Further scale-up fermentation followed by chemical investigation of the metabolites of this co-culture system yielded six new compounds, phomretones A–F (**1–6**) (Fig. 1), which were a series of structurally related C_{12} polyketides that differ in the geometry and substitution pattern. Notably, LC-MS analysis confirmed these metabolites were not detected in the culture broth of *Phoma* sp. YUD17001 or *Armillaria* sp., but were only produced during co-cultivation (Fig. S2 and S3, ESI†). Herein are reported the isolation, structure elucidation, and bioactivity evaluation for all of these compounds.

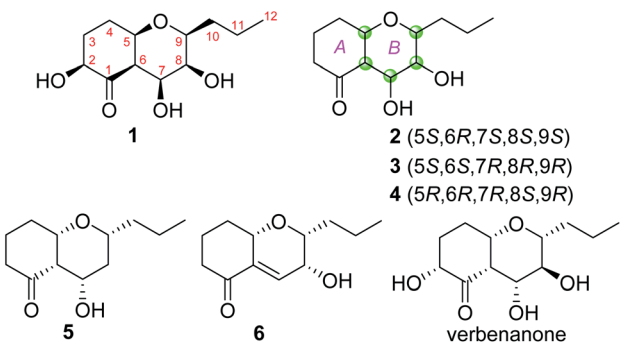

Fig. 1 Chemical structures of compounds **1–6** and verbenanone.

Results and discussion

Phomretone A (**1**) was obtained as a colorless solid. A molecular formula of $C_{12}H_{20}O_5$ was assigned by interpretation of HREIMS. The IR spectrum showed absorption bands at 3340 and 1721 cm^{-1} indicating the presence of hydroxyl and carbonyl groups. The 1D NMR data (Tables 1 and 2) of **1** revealed one methyl group, four methylenes, six methines including five oxygenated, and one nonprotonated carbon. Interestingly, these data were similar to those for a recently reported novel polyketide, verbenanone, described by Chunshun Li *et al.*[14] The major difference was the C-1, C-3, C-5, C-7, and C-9 signals of compound **1** were upfield ($\Delta\delta_C$ −4.0, −2.0, −4.7, −8.7, and

Key Laboratory of Functional Molecules Analysis and Biotransformation of Universities in Yunnan Province, Key Laboratory of Medicinal Chemistry for Natural Resource, Ministry of Education, School of Chemical Science and Technology, Yunnan University, Kunming 650091, China. E-mail: haozhou@ynu.edu.cn; ztding@ynu.edu.cn

† Electronic supplementary information (ESI) available: 1D and 2D NMR, HRESIMS, HPLC-MS, and UV spectra of phomretones A–F, along with other details. See DOI: 10.1039/d0ra02524k

Table 1 ^{1}H NMR data for compounds **1–6** (δ in ppm, J values in Hz)[a]

No.	1	2	3	4	5	6
1						
2	4.16, dd (12.4, 6.8)	2.30, m	2.42, m	2.44, overlap	2.40, m	2.49, d (18.0)
			2.26, m	2.26, m	2.26, m	2.31, m
3	2.22, m	2.00, m	2.02, overlap	2.02, m	2.03, overlap	1.98, m
	1.47, overlap	1.56, overlap	1.88, overlap	1.53, overlap	1.86, overlap	1.73, m
4	2.13, m	2.13, m	2.03, overlap	2.11, m	2.01, overlap	2.16, m
	1.79, m	1.70, m	1.86, overlap	1.77, m	1.85, overlap	1.56, overlap
5	3.79, dt (10.8, 4.0)	3.79, m	4.32, m	3.23, m	4.34, br s	4.26, m
6	2.48, d (10.8)	2.48, m	2.80, m	2.46, overlap	2.52, br s	
7	4.35, br s	4.36, br s	4.37, m	3.76, m	4.46, m	6.46, br s
8	3.14, dd (9.6, 2.4)	3.14, dd (9.6, 3.2)	3.32, m	3.08, overlap	1.51, m	3.92, m
9	3.54, m	3.53, m	3.49, m	3.10, overlap	3.72, m	3.26, m
10	1.79, overlap	1.79, m	1.70, m	1.80, m	1.40, overlap	1.82, m
	1.37, overlap	1.37, overlap	1.32, overlap	1.37, overlap	1.29, overlap	1.42, overlap
11	1.57, overlap	1.59, overlap	1.51, m	1.56, overlap	1.39, overlap	1.60, overlap
	1.36, overlap	1.36, overlap	1.31, overlap	1.36, overlap	1.32, overlap	1.42, overlap
12	0.93, t (7.2)	0.93, t (7.2)	0.91, t (7.2)	0.93, t (7.2)	0.90, t (6.8)	0.96, t (7.2)

[a] Measured at 400 MHz in methanol-d_4.

Table 2 ^{13}C NMR data for compounds **1–6** (δ in ppm)[a]

No.	1	2	3	4	5	6
1	208.4, C	210.1, C	212.4, C	210.1, C	212.7, C	201.3, C
2	75.7, CH	41.2, CH_2	42.5, CH_2	41.9, CH_2	42.6, CH_2	40.5, CH_2
3	30.8, CH_2	21.5, CH_2	22.7, CH_2	22.6, CH_2	22.6, CH_2	19.6, CH_2
4	29.7, CH_2	31.6, CH_2	30.7, CH_2	32.2, CH_2	31.4, CH_2	31.7, CH_2
5	74.7, CH	74.5, CH	74.4, CH	79.9, CH	74.9, CH	76.9, CH
6	57.5, CH	59.5, CH	57.3, CH	62.1, CH	55.5, CH	141.8, C
7	66.9, CH	66.7, CH	67.6, CH	72.1, CH	64.3, CH	135.7, CH
8	73.2, CH	73.5, CH	69.7, CH	76.3, CH	36.1, CH_2	68.7, CH
9	76.4, CH	76.4, CH	77.1, CH	80.8, CH	73.5, CH	79.7, CH
10	35.2, CH_2	35.2, CH_2	35.3, CH_2	35.1, CH_2	39.4, CH_2	35.7, CH_2
11	19.6, CH_2	19.6, CH_2	19.3, CH_2	19.6, CH_2	19.5, CH_2	19.8, CH_2
12	14.5, CH_3	14.5, CH_3	14.5, CH_3	14.4, CH_3	14.5, CH_3	14.4, CH_3

[a] Measured at 100 MHz in methanol-d_4.

−5.5, respectively) when compared with verbenanone, whereas C-6 and C-8 of **1** were shifted downfield ($\Delta\delta_C$ +2.3 and +0.5). Subsequently, following detailed inspection of the ^{1}H–^{1}H COSY and HMBC data (Fig. 1) of **1**, its planar structure was determined as being the same as that of verbenanone, suggesting that **1** might be a stereoisomer of verbenanone.[14] The relative configuration of **1** was established based on the ROESY correlations as indicated in Fig. 2. The ROESY spectrum showed cross-peaks of H-2/H-6, H-5/H-6, H-5/H-9, H-6/H-7/H-8, and H-8/H-9 indicating that H-5, H-6, and H-9 were on the same side and assigned in the α-position, whereas 2-OH, 7-OH, and 8-OH were β-oriented. The absolute configuration of **1** was elucidated by comparing the quantum chemical calculations of the calculated electronic circular dichroism (ECD) spectra at the B3LYP/6-31G(d,p) level in methanol with the experimental one. The calculated ECD curve of the (2*S*,5*R*,6*R*,7*S*,8*S*,9*S*)-enantiomer showed the identical Cotton effects (CEs) as the experimental ECD curve for **1** (Fig. 3A). Therefore, the absolute configuration of **1** was assigned as 2*S*, 5*R*, 6*R*, 7*S*, 8*S*, 9*S*, and **1** was identified as the stereoisomer of verbenanone.[14]

Phomretones B (**2**), C (**3**), and D (**4**) were also isolated as colorless solids. Their HRESIMS data established the identical molecular formula of $C_{12}H_{20}O_4$ ($[M + Na]^+$ m/z 251.1251,

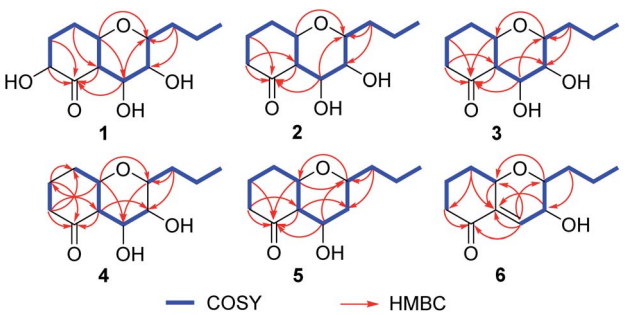

Fig. 2 Key ^{1}H–^{1}H COSY and HMBC correlations of **1–6**.

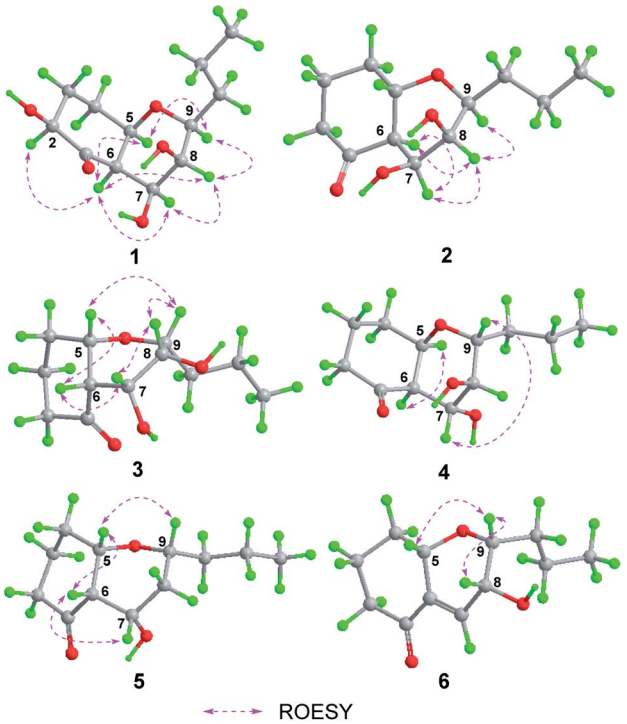

Fig. 3 Conformations and key ROESY correlations of **1–6**.

251.1254, and 251.1253, respectively). Comparison of the ^{13}C NMR data (Table 2) of **2–4** suggested that three compounds possess similar carbon chemical shifts. Markedly, notable differences were observed for resonances attributable to the B ring with chiral carbon signals, which could be influenced by the different spatial configurations of C-5, C-6, C-7, C-8, and C-9 (Fig. 5). Furthermore, their ^{1}H and ^{13}C NMR data (Tables 1 and 2) showed considerable resemblance to that of **1**. The main difference between compounds **2–4** and **1** was the lack of an oxygenated methine signal (δ_H 4.16, δ_C 75.7), suggesting the absence of a hydroxyl group at C-2 in **2–4**. This was ascertained with the DEPT and 2D NMR experiments (ESI†). The key ^{1}H–^{1}H COSY and HMBC correlations observed for **2–4** (Fig. 2) showed that the three compounds share identical constitution atomic arrangement, being stereoisomers of each other. This was further supported by comparison of the ROESY data (Fig. 3) of **2–4**. For **2**, the key ROESY correlations of H-6/H-7/H-8 and H-8/H-9 supported their β-orientation. In contrast, H-5 was assigned to α-orientation. For compound **3**, the β-orientations of H-5, H-6, H-7, H-8, and H-9 was inferred through ROESY correlations of H-5/H-6/H-7/H-8/H-9. Moreover, the relative configuration of **4** was determined as shown (Fig. 3). The ROESY correlation of H-5/H-6 suggested that H-5 and H-6 are α-oriented. The β-orientations assigned to H-7 and H-9 were supported by the ROESY cross-peaks of H-7/H-9. To verify the above structural assignment and to determine the absolute configurations of **2–4**, the ECD calculation was performed, together with comparison of the CEs in the calculated and experimental curves (Fig. 4B–D). On the basis of the above, the absolute configurations of compounds **2–4** were deduced to be (5*S*,6*R*,7*S*,8*S*,9*S*), (5*S*,6*S*,7*R*,8*R*,9*R*), and (5*R*,6*R*,7*R*,8*S*,9*R*), respectively.

Phomretone E (**5**) exhibited a molecular formula of $C_{12}H_{20}O_3$, which was one oxygen atom mass unit less than that of **2**. Its 1D NMR spectroscopic data (Tables 1 and 2) were highly similar to those of **2**, except that an oxygenated methine (δ_H 3.16, δ_C 73.5) was absent and a methylene signal at C-8 (δ_H 1.51, δ_C 36.1) was present in **5**. Combined with the molecular mass information, **5** was identified to be a deoxy analogue of **2**.

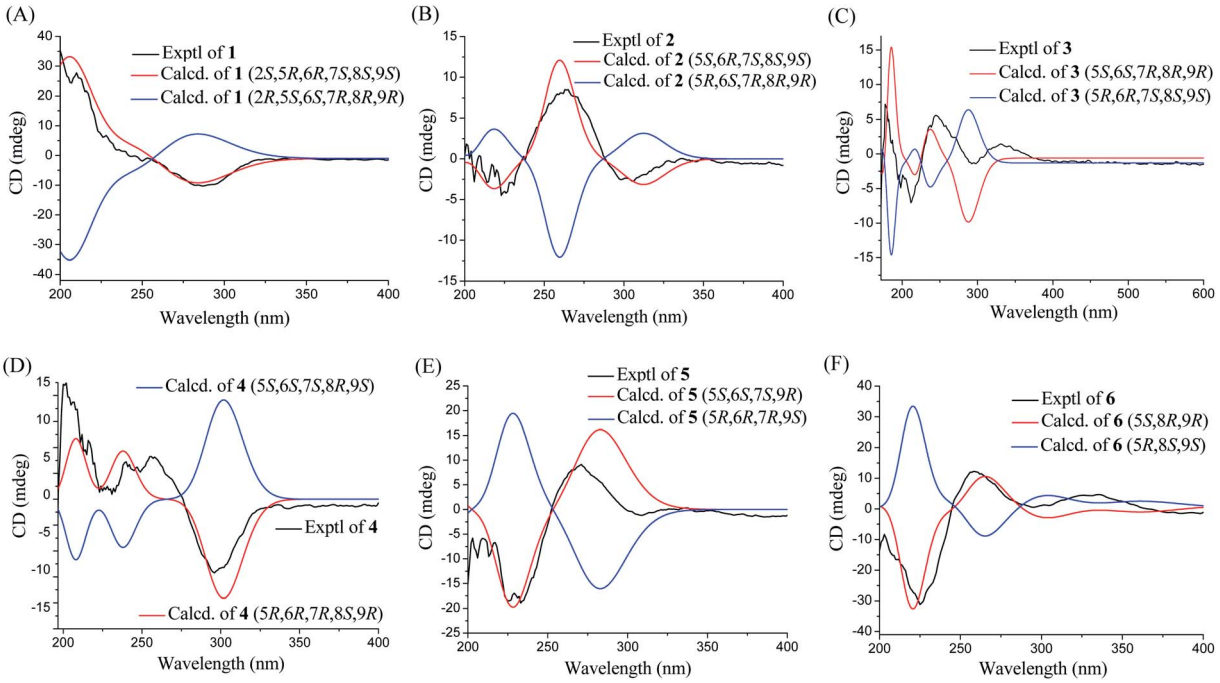

Fig. 4 Experimental and calculated ECD spectra of compounds **1–6** (A–F).

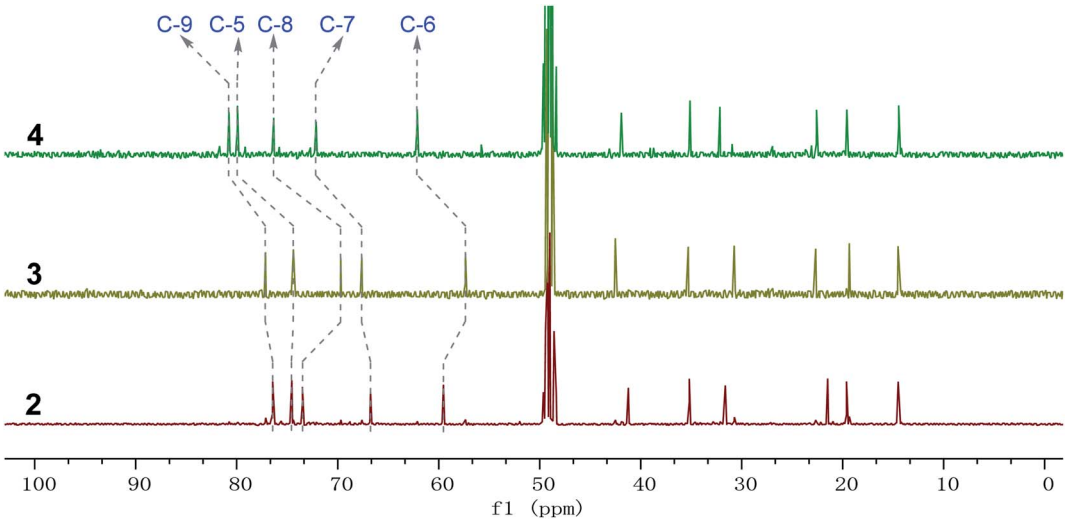

Fig. 5 Comparison of ^{13}C NMR spectra of compounds **2–4** from δ_C 0 to 100 ppm; **2–4** possess similar carbon chemical shifts; the major deviations among **2–4** are the chiral carbon signals C-5, C-6, C-7, C-8, and C-9, respectively.

Further analyses of NMR data, including COSY, HMBC, and ROESY experiments (Fig. 2 and 3), yielded the planar structure and relative configuration of **5**. Additionally, the calculated ECD curve for the (5*S*,6*S*,7*S*,9*R*)-enantiomer (Fig. 4E) coincided well with the experimental data of **5**. Accordingly, the structure of **5** was defined as shown in Fig. 1.

Phomretone F (**6**) was purified as a colorless solid, and its molecular formula was determined as $C_{12}H_{18}O_3$ on the basis of HRESIMS data, corresponding to four degrees of unsaturation. Its 1D NMR data (Tables 1 and 2) resembled those of **3**, with the exception of the presence of an additional trisubstituted double bond [δ_H 6.46 (1H, br s, H-7); δ_C 141.8 (C-6), 135.7 (C-7)] and the absence of one hydroxyl group in **6**. Further analysis of the HMBC correlations from H-5 (δ_H 4.26) and H-7 (δ_H 6.46) to C-6 (δ_C 141.8), and from H-7 (δ_H 6.46) to C-9 (δ_C 79.7) indicated the location of the double bond between C-6 and C-7. The ROESY experiment (Fig. 3) showed correlations between H-5 and H-9 as well as between H-8 and H-9, which revealed the H-5, H-8, and H-9 all to be in a β-orientation relative configuration. As shown in Fig. 4F, the calculated ECD spectrum for (5*S*,8*R*,9*R*)-**6** matched well with the experimental ECD spectrum, which elucidated the absolute configuration of **6** as 5*S*, 8*R*, 9*R*.

All isolated compounds (**1–6**) were tested in cytotoxicity, anti-acetylcholinesterase, and anti-PTP1B enzyme assays, but none showed significant inhibitory activities (details see ESI†).

Conclusions

In summary, there was no evidence of the production of the phomretones A–F by either fungus when grown as axenic cultures, which may be a result of the co-culture of *Phoma* sp. YUD17001 with *Armillaria* sp. Consequently, the present study may serve as a further example of the successful application of co-culture approaches for expanding the metabolic profile of microorganisms. Furthermore, the study will provide an opportunity to deepen the understanding of the interactions among the fungal community associated with *G. elata* habitats and their relationship with the host plant.

Experimental section

General experimental procedures

Optical rotation, UV, and IR data were obtained using JASCO P-1020 polarimeter, Shimadzu UV2401PC, and Bruker Tensor-27 with KBr pellets, respectively. CD spectra were recorded on an Applied Photophysics digital circular dichroism chiroptical spectrometer (Surrey, UK). 1D and 2D NMR spectra were recorded in methanol-d_4 using tetramethylsilane as internal standard on a Bruker DRX-400 MHz spectrometer (Bruker Co., Karlsruhe, Germany). HRESIMS was performed using an Agilent G3250AA Q-TOF MS (Agilent, Santa Clara, CA, USA). Preparative HPLC was performed on an Agilent 1260 series equipped with a DAD detector and a Zorbax SB-C_{18} (250 × 9.4 mm, 5 μm) semipreparative column. Silica gel (200–300 mesh), Sephadex™ LH-20 gel (Uppsala, Sweden), and RP-C_{18} silica gel (150–200 mesh, Merck) were used for column chromatography (CC). Fractions were monitored by TLC (GF_{254}, Qingdao Haiyang Chemical Co. Ltd), with spots were detected by spraying with 10% H_2SO_4 in ethanol, followed by heating.

Fungal material

Identification of two fungi (*Phoma* sp. YUD17001 and *Armillaria* sp.) was based on sequence data analysis of the internal transcribed spacer (ITS) regions of the 18S rRNA (GenBank accession numbers MH665638 and MK079569, respectively). More details about the experimental procedures are provided in work described previously.[11]

Co-culture conditions

Scale-up liquid co-cultures of *Phoma* sp. YUD17001 and *Armillaria* sp. were performed according to the previously reported method.[11]

Extraction and isolation

The whole co-cultures (50 L) were separated from the mycelium by vacuum filtration and partitioned with ethyl acetate (EtOAc) three times. The extract was evaporated under reduced pressure, yielding 11.0 g of brown extract. The extract was subjected to silica gel CC with a $CHCl_3$–MeOH gradient system (100 : 0, 50 : 1, 30 : 1, 10 : 1, 1 : 1, and 0 : 100 v/v) to yield six fractions (A–F). Fraction B was further submitted to Sephadex LH-20 gel CC ($CHCl_3$–MeOH, 1 : 1 v/v), and was pooled according to TLC analysis data to afford four combined subfractions (B1–B4). Elution of B1 with petroleum ether (PE)–EtOAc (9 : 1 and 3 : 1 v/v) afforded **5** (6.4 mg). Fraction B3 was divided into three portions (B3.1–B3.3) by silica gel CC (PE–EtOAc, 20 : 1–5 : 1 v/v) to obtain further fractions. Fraction B3.2 was fractionated by RP-C_{18} CC (MeOH–H_2O, 1 : 4–3 : 2 v/v) to yield **2** (9.0 mg), **3** (7.8 mg), and **4** (2.0 mg). Compound **6** (t_R = 26 min, 2.5 mg) was isolated by fractionation of B4 using semipreparative HPLC (MeOH–H_2O, 7 : 3 v/v). Fraction C was further fragmented by RP-C_{18} CC (MeOH–H_2O, 1 : 9–1 : 0 v/v) to yield five subfractions (C1–C5). Purification of C2 over Sephadex LH-20 (MeOH) gave **1** (3.2 mg).

Phomretone A (1). Colorless solid; $[\alpha]_D^{23}$ +8.4 (*c* 0.32, MeOH); UV (MeOH) λ_{max} (log ε) 228 (0.29), 267 (0.24) nm; IR (KBr) ν_{max} 3340, 2956, 2870, 1721, 1358, 1252 cm^{-1}; ^1H and ^{13}C NMR data see Tables 1 and 2; HRESIMS *m*/*z* 267.1208 $[M + Na]^+$ (calcd for $C_{12}H_{20}O_5Na$, 267.1203).

Phomretone B (2). Colorless solid; $[\alpha]_D^{23}$ +34.3 (*c* 0.24, MeOH); UV (MeOH) λ_{max} (log ε) 232 (0.50) nm; IR (KBr) ν_{max} 3335, 2955, 2878, 1728, 1374, 1250 cm^{-1}; ^1H and ^{13}C NMR data see Tables 1 and 2; HRESIMS *m*/*z* 251.1251 $[M + Na]^+$ (calcd for $C_{12}H_{20}O_4Na$, 251.1254).

Phomretone C (3). Colorless solid; $[\alpha]_D^{23}$ +39.8 (*c* 0.41, MeOH); UV (MeOH) λ_{max} (log ε) 231 (0.53) nm; IR (KBr) ν_{max} 3335, 2953, 2878, 1726, 1374, 1253 cm^{-1}; ^1H and ^{13}C NMR data see Tables 1 and 2; HRESIMS *m*/*z* 251.1254 $[M + Na]^+$ (calcd for $C_{12}H_{20}O_4Na$, 251.1254).

Phomretone D (4). Colorless solid; $[\alpha]_D^{23}$ +33.6 (*c* 0.22, MeOH); UV (MeOH) λ_{max} (log ε) 253 (0.63) nm; IR (KBr) ν_{max} 3336, 2955, 2870, 1723, 1358, 1253 cm^{-1}; ^1H and ^{13}C NMR data see Tables 1 and 2; HRESIMS *m*/*z* 251.1253 $[M + Na]^+$ (calcd for $C_{12}H_{20}O_4Na$, 251.1254).

Phomretone E (5). Colorless solid; $[\alpha]_D^{23}$ −14.8 (*c* 0.14, MeOH); UV (MeOH) λ_{max} (log ε) 245 (0.78) nm; IR (KBr) ν_{max} 3334, 2956, 2870, 1723, 1358, 1254 cm^{-1}; ^1H and ^{13}C NMR data see Tables 1 and 2; HRESIMS *m*/*z* 235.1304 $[M + Na]^+$ (calcd for $C_{12}H_{20}O_3Na$, 235.1305).

Phomretone F (6). Colorless solid; $[\alpha]_D^{23}$ +60.1 (*c* 0.11, MeOH); UV (MeOH) λ_{max} (log ε) 241 (2.14) nm; IR (KBr) ν_{max} 3335, 2955, 2880, 1723, 1653, 1378, 1252 cm^{-1}; ^1H and ^{13}C NMR data see Tables 1 and 2; HRESIMS *m*/*z* 209.1183 $[M - H]^-$ (calcd for $C_{12}H_{17}O_3$, 209.1183).

TDDFT-ECD calculations

The conformational search for the molecule was carried out using the MMFF94S force field and CONFLEX software.[15] The stable conformers with relative energy within a 5.0 kcal mol^{-1} energy window were obtained. The conformers obtained were further optimized with the software package Gaussian 09. Methanol was used as a solvent with the polarizable continuum solvent model (PCM). Time dependent density functional theory (TDDFT) at the B3LYP/6-311+G(d,p) level in the gas phase was used for ECD calculations.[16,17] Boltzmann statistics were applied for the final simulations of the ECD spectra. These steps were performed with the software SpecDis1.64.[18]

HPLC-MS analysis

LC-MS experiments were carried out by the detector of Agilent G3250AA Q-TOF mass spectrometer with electrospray ionization (ESI) source. The data were acquired in the scan mode at *m*/*z* 100–1000 in the positive ionization mode. Chromatography was performed using a Zorbax Eclipse XDB-C_{18} column (150 × 2.1 mm, 5 μm) with a H_2O (A)/MeCN (B) gradient at a flow rate of 0.5 mL min^{-1}. The injection volume was set to 2 μL (concentration of 0.5 mg mL^{-1}). The solvent gradient time program was as follows: initial 10% B, then linear increase to 40% at 25 min, 65% at 35 min, 85% at 45 min, 95% at 55 min, and hold for 5 min before returning to starting conditions.

Cytotoxicity assay

The *in vitro* cytotoxicity of compounds **1–6** was assessed by 3-(4,5-dimethylthiazol-2-yl)-5(3-carboxymethoxyphenyl)-2-(4-sulfophenyl)-2*H*-tetrazolium (MTS) assay on five human cancer cell lines (HL-60, A-549, SMMC-7721, MCF-7, and SW480) performed,[19,20] and cisplatin was used as a positive control. The cells were seeded onto 96-well plates at 2 × 10^4 cells per well and after 24 h the compounds were added in different concentrations. Subsequently, MTS was added to the culture medium and the absorbance at 490 nm was measured with a microplate reader. The proliferation rate was calculated as the ratio of absorbance to that of the control.

AChE inhibitory assay

Inhibitory activities of compounds **1–6** on AChE enzyme were determined by using modified Ellman's method as described in a previous study.[12]

PTP1B inhibitory bioassay

PTP1B activity was determined by measuring the rate of hydrolysis of a surrogate substrate, *p*-nitrophenyl phosphate.[21,22]

Conflicts of interest

There are no conflicts to declare.

Acknowledgements

This work was financially supported by grants from the Natural Science Foundation of China (No. 81603005 and 81860623), a project of Yunling Scholars of Yunnan Province, the Program for Changjiang Scholars and Innovative Research Team in University (IRT_17R94).

Notes and references

1 R. Sugiyama, S. Nishimura, T. Ozaki, S. Asamizu, H. Onaka and H. Kakeya, *Angew. Chem., Int. Ed.*, 2016, **128**, 10434–10438.
2 S. Bertrand, N. Bohni, S. Schnee, O. Schumpp, K. Gindro and J. L. Wolfender, *Biotechnol. Adv.*, 2014, **32**, 1180–1204.
3 N. Adnani, S. R. Rajski and T. S. Bugni, *Nat. Prod. Rep.*, 2017, **34**, 784–814.
4 G. Yu, Z. Sun, J. Peng, M. Zhu, Q. Che, G. Zhang, T. Zhu, Q. Gu and D. Li, *J. Nat. Prod.*, 2019, **82**, 2013–2017.
5 M. Moussa, W. Ebrahim, M. Bonus, H. Gohlke, A. Mándi, T. Kurtán, R. Hartmann, R. Kalscheuer, W. Lin, Z. Liu and P. Proksch, *RSC Adv.*, 2019, **9**, 1491–1500.
6 W. Wang, F. Zeng, Q. Bie, C. Dai, C. Chen, Q. Tong, J. Liu, J. Wang, Y. Zhou, H. Zhu and Y. Zhang, *Org. Lett.*, 2018, **20**, 6817–6821.
7 A. Stierle, D. Stierle, D. Decato, N. Priestley, J. Alverson, J. Hoody, K. McGrath and D. Klepacki, *J. Nat. Prod.*, 2017, **80**, 1150–1160.
8 D. Oh, P. Jensen, C. Kauffman and W. Fenical, *Bioorg. Med. Chem.*, 2005, **13**, 5267–5273.
9 S. Huang, W. Ding, C. Li and D. G. Cox, *Pharmacogn. Mag.*, 2014, **40**, 410–414.
10 L. Meng, Y. Liu, X. Li, G. Xu, N. Ji and B. Wang, *J. Nat. Prod.*, 2015, **78**, 2301–2305.
11 H. T. Li, H. Zhou, R. T. Duan, H. Y. Li, L. H. Tang, X. Q. Yang, Y. B. Yang and Z. T. Ding, *J. Nat. Prod.*, 2019, **82**, 1009–1013.
12 H. T. Li, L. Tang, T. Liu, R. Yang, Y. Yang, H. Zhou and Z. T. Ding, *Org. Chem. Front.*, 2019, **6**, 3847–3853.
13 H. T. Li, L. H. Tang, T. Liu, R. N. Yang, Y. B. Yang, H. Zhou and Z. T. Ding, *Bioorg. Chem.*, 2020, **95**, 103503.
14 C. Li, A. M. Sarotti, J. Turkson and S. Cao, *Tetrahedron Lett.*, 2017, **58**, 2290–2293.
15 B. Jagannadh, S. S. Reddy and R. Thangavelu, *J. Mol. Model.*, 2004, **10**, 55–59.
16 N. Berova, L. Di Bari and G. Pescitelli, *Chem. Soc. Rev.*, 2007, **36**, 914–931.
17 G. Bringmann, T. Bruhn, K. Maksimenka and Y. Hemberger, *Eur. J. Org. Chem.*, 2009, 2717–2727.
18 T. Bruhn, A. Schaumlöffel and Y. Hemberger, *SpecDis, version 1.64*, University of Wüerzburg, Germany, 2015.
19 A. H. Cory, T. C. Owen, J. A. Barltrop and J. G. Cory, *Cancer Commun.*, 1991, **3**, 207–212.
20 Y. Ren, J. C. Gallucci, X. Li, L. Chen, J. Yu and A. D. Kinghorn, *J. Nat. Prod.*, 2018, **81**, 554–561.
21 M. K. Mahapatra, R. Kumar and M. Kumar, *Bioorg. Chem.*, 2017, **71**, 1–9.
22 F. F. Liu, T. Yuan, W. Liu, H. Ma, N. P. Seeram, Y. Li, L. Xu, Y. Ma, X. Huang and L. Li, *J. Nat. Prod.*, 2017, **80**, 544–550.